Published in final edited form as:
Nat Med. ; 17(10): 1275–1282. doi:10.1038/nm.2459.

Tumor suppressor BRCA1 epigenetically controls oncogenic microRNA-155

Suhwan Chang[1], **Rui-Hong Wang**[2], **Keiko Akagi**[3], **Kyung-Ae Kim**[1], **Betty K Martin**[4], **Luca Cavallone**[5,6], **Kathleen Cuningham Foundation Consortium for Research into Familial Breast Cancer (kConFab)**[7], **Diana C Haines**[8], **Mark Basik**[5], **Phuong Mai**[9], **Elizabeth Poggi**[10], **Claudine Isaacs**[10], **Lai M Looi**[11], **Kein S Mun**[11], **Mark H Greene**[9], **Stephen W Byers**[10], **Soo H Teo**[12,13], **Chu-Xia Deng**[2], and **Shyam K Sharan**[1]

[1]Mouse Cancer Genetics Program, Center for Cancer Research, National Cancer Institute at Frederick, Frederick, Maryland, USA

[2]Genetics of Development and Disease Branch, National Institute of Diabetes and Digestive and Kidney Diseases, Bethesda, Maryland, USA

[3]Human Cancer Genetics Program, Departments of Molecular Virology, Immunology and Medical Genetics, Ohio State University, Columbus, Ohio, USA

[4]SAIC-Frederick, National Cancer Institute at Frederick, Frederick, Maryland, USA

[5]Lady Davis Institute, Jewish General Hospital, Montréal, Quebec, Canada

[6]Program in Cancer Genetics, Departments of Oncology and Human Genetics, McGill University, Montréal, Quebec, Canada

[7]The Peter MacCallum Cancer Centre, East Melbourne, Victoria, Australia

[8]Pathology Histotechnology Laboratory, SAIC-Frederick, National Cancer Institute at Frederick, Frederick, Maryland, USA

[9]Clinical Genetics Branch, National Cancer Institute, Rockville, Maryland, USA

[10]Georgetown- Lombardi Comprehensive Cancer Center Georgetown University, Washington, DC, USA

[11]Department of Pathology, University Malaya Medical Center, Kuala Lumpur, Malaysia

[12]Department of Surgery University Malaya Cancer Research Institute, University Malaya Medical Centre, Kuala Lumpur, Malaysia

[13]Cancer Research Initiatives Foundation, Sime Darby Medical Centre, Kuala Lumpur, Malaysia

Abstract

Correspondence should be addressed to S.K.S. (sharans@mail.nih.gov).

Note: Supplementary information *is available on the* Nature Medicine *website.*

AUTHOR CONTRIBUTIONS

S.C. conceived the idea, conducted all the experiments and wrote the manuscript, R.H.W. and C.X.D. helped with xenograft experiment, provided mouse tumor samples and cell lines, K.A. carried out bioinformatics analysis, K.A.K. helped with experiments, B.K.M. helped with mouse work, D.C.H. performed histopathological analysis, L.C. analyzed human tumor samples, M.B., P.M., M.H.G., KConFab, L.M.L., K.S.M., S.H.T., E.P., C.I. and S.W.B provided human tumor samples, S.K.S. conceived the idea, supervised the study and wrote the manuscript.

COMPETING FINANCIAL INTERESTS

The authors declare no competing financial interests.

BRCA1, a well-known tumor suppressor with multiple interacting partners, is predicted to have diverse biological functions. However, so far its only well-established role is in the repair of damaged DNA and cell cycle regulation. In this regard, the etiopathological study of low-penetrant variants of BRCA1 provides an opportunity to uncover its other physiologically important functions. Using this rationale, we studied the R1699Q variant of BRCA1, a potentially moderate-risk variant, and found that it does not impair DNA damage repair but abrogates the repression of microRNA-155 (miR-155), a bona fide oncomir. Mechanistically, we found that BRCA1 epigenetically represses miR-155 expression via its association with HDAC2, which deacetylates histones H2A and H3 on the miR-155 promoter. We show that overexpression of miR-155 accelerates whereas the knockdown of miR-155 attenuates the growth of tumor cell lines *in vivo*. Our findings demonstrate a new mode of tumor suppression by BRCA1 and suggest that miR-155 is a potential therapeutic target for BRCA1-deficient tumors.

The protein encoded by human breast cancer susceptibility gene *BRCA1* is involved in DNA damage repair and cell cycle progression[1–3]. BRCA1 has two distinct functional domains: the N-terminal RING domain binds to BARD1 and has E3 ubiquitin ligase activity[4,5], whereas the C-terminal BRCT domain is essential for transcriptional regulation and DNA double-strand break repair (DSBR) function[6–10]. After phosphorylation by ATM, ATR, Aurora A and Cdk2 kinase, BRCA1 localizes to the site of damaged DNA[11–14]. Mutations in *BRCA1* are associated with substantially increased risk of developing breast and ovarian cancer[15].

In this study, we characterized the R1699Q point mutation in the BRCT domain (ex.18:c. 5095G>A, p.R1699Q). Arg1699 is predicted to be critical for the formation of hydrogen bonds with DNA helicase BACH1 phosphopeptide[16]. R1699Q does not completely destabilize the phosphopeptide interaction, but may cause loss of phosphospecificity [17]. R1699Q has been associated with predisposition to breast cancer but the precise risk is unknown [18,19].

Using a mouse embryonic stem cell (ES cell)-based functional assay[20], we found that R1699Q did not affect genomic stability or cause any apparent cell cycle defects. However, R1699Q ES cells undergoing differentiation upregulated an oncogenic microRNA, miR-155. In humans, miR-155 is transcribed from the MIR155HG gene (also known as the B-cell integration cluster or BIC locus and referred to hereafter as miR-155) that encodes a noncoding RNA and is a proviral insertion site of the avian leukosis virus[21]. Functional studies of mir-155 in mice and its upregulation in many types of B-cell lymphoma and myeloid leukemia suggest it is oncogenic[22–26]. A recent study has shown that miR-155 has mutator activity[27]. Several known targets of miR-155 are involved in apoptotic and/or proliferative response and contribute to tumor development[28–30]. Here, we demonstrate a previously unknown role for BRCA1 in the epigenetic control of miR-155.

RESULTS

R1699Q variant affects ES cell survival and differentiation

Previously, we developed a mouse ES cell-based assay and used it to examine the functional significance of the 13 BRCA1 variants[20]. The assay is based on the ability of human *BRCA1* transgene cloned in a bacterial artificial chromosome (BAC) vector to complement the loss of endogenous *Brca1* in mouse ES cells (PL2F8) that contain a conditional allele of *Brca1* (Fig. 1a). Using this assay, we observed ten-fold lower survival of R1699Q BRCA1–expressing $Brca1^{ko/ko}$ ES cells compared with wild-type *BRCA1* (Fig. 1b). The deleterious nature of this variant was further supported by its inability to rescue the embryonic lethality of *Brca1*-null mice (Supplementary Fig. 1a–c).

R1699Q ES cells (*Brca1*$^{ko/ko}$, rescued by R1699Q BRCA1) had no substantial defects in sensitivity to DNA damaging agents, cell growth or overall genomic stability (Supplementary Fig. 2a–h). To determine the effect of R1699Q mutation, we differentiated the ES cells into embryoid bodies that represent an *in vitro* model of early embryogenesis (Fig. 1c). Histological analysis of R1699Q embryoid bodies showed lack of the outer primitive endodermal layer (Fig. 1d); this was corroborated by reduced mRNA levels of *Lamb1* an endodermal marker (Supplementary Fig. 3a). The cells of the outer layer of the R1699Q embryoid bodies were TUNEL^{+} (Fig. 1e), suggesting that the absence of the primitive endodermal layer is due to apoptotic cell death. The inner layers of the R1699Q embryoid bodies were composed mainly of mesodermal cells (mesodermal marker *T*, also known as Brachyury was highly upregulated; Supplementary Fig. 3b), unlike the wild-type embryoid bodies, which had distinct cell layers (Fig. 1d). We confirmed that these defects were not due to genomic instability in the differentiating cells (data not shown). R1699Q ES cells also exhibited defects during *in vivo* differentiation into teratomas. Compared with wild-type ES cells, R1699Q ES cells formed teratomas significantly more slowly (Fig. 1f) and had fewer neurorosette structures comprised of poorly differentiated, rapidly growing neural cells (Fig. 1g).

To understand the difference between wild-type and R1699Q embryoid bodies at the molecular level, we carried out comparative gene expression profiling (Supplementary Table 1) and found several altered signaling pathways including those related to stem cell differentiation (Supplementary Table 2). Additionally, R1699Q embryoid bodies had two-fold lower concentrations of stem cell marker *Nanog* compared with wild-type cells (Supplementary Fig. 3c), although another marker, *Pou5f1* (also known as *Oct-4*), showed no difference (Supplementary Fig. 3d). These data are consistent with the hypothesis that R1699Q ES cells are prone to spontaneous differentiation, possibly explaining the ten-fold reduction in their survival.

miR-155 is upregulated in R1699Q mutant cells

Dicer1-null ES cells have a very similar phenotype to that of the R1699Q ES cells, including deregulated embryoid body formation and defective teratoma growth[31]. Because Dicer is a key enzyme involved in maturation of microRNA (miRNA), this phenotypic similarity led us to investigate whether miRNA expression is misregulated in wild-type and R1699Q embryoid bodies. As an additional control, we examined embryoid bodies generated from ES cells expressing M1652I BRCA1, a neutral variant that is functionally indistinguishable from wild-type BRCA1 (refs. 20,32). We identified a single miRNA, miR-155, to be consistently upregulated (more than two-fold) in R1699Q cells (Supplementary Table 3). miR-155 is an oncogenic miRNA that is upregulated in many cancers, including breast cancer[33,34]. We confirmed miR-155 upregulation in R1699Q cells by real-time PCR (rtPCR; Fig. 2a). *In situ* hybridization revealed ~40-fold upregulation of miR-155 (Fig. 2b) in a subset of the cells from R1699Q embryoid bodies.

We next tested whether the upregulation of miR-155 was the cause or the result of the differentiation defects observed in the R1699Q ES cells. Using a tet-inducible system we overexpressed miR-155 in wild-type ES cells (Fig. 2c,d). miR-155 overexpression during embryoid body and teratoma formation led to a phenotype similar to those observed in R1699Q ES cells (Fig. 2e–g). H&E-stained control embryoid bodies are not exactly like wild-type embryoid bodies (Fig. 2e), probably due to leaky expression of miR-155. These results suggest that miR-155, at least in part, contributed to the differentiation defects observed in R1699Q ES cells.

miR-155 is upregulated in BRCA1-deficient cell

The upregulation of miR-155 in R1699Q cells suggests that BRCA1 controls its expression. To test this possibility, we measured miR-155 expression in tumors from *Brca1*$^{ko/+}$;*Trp53*$^{ko/+}$;*Tg*^{R1699Q} mice, which have *Brca1* and *Trp53* knockout alleles on the same chromosome (S.C. and S.K.S, unpublished data). Of the nine tumors we tested, eight had 30- to 180-fold upregulation of miR-155 compared with normal tissues (Fig. 3a and Supplementary Table 4). The one tumor (RQ163) that did not highly express miR-155 (Fig. 3a) retained the wild-type *Brca1* allele, whereas six of the seven tumors with greater miR-155 expression than normal tissues showed loss of wild-type *Brca1* (Supplementary Fig. 4a), suggesting that loss of wild-type *Brca1* is required for miR-155 upregulation. Notably, four tumors from *Brca1*$^{ko/+}$;*Trp53*$^{ko/+}$;*Tg*^{M1652I} mice showed only marginal increase in miR-155. miR-155 was also upregulated in a tumor from an R1699Q mutation carrier, although the magnitude of increase was smaller (Fig. 3b; see Discussion). This tumor also exhibited a reduction in the copy number of *BRCA1,* suggesting a possible *BRCA1* loss of heterozygosity (LOH) (Supplementary Fig. 4b).

Next, we tested a panel of human breast cancer cell lines with different *BRCA1* genotypes to examine whether the deregulation of miR-155 is specific to R1699Q or whether the complete loss of BRCA1 has a similar effect. Northern blotting and rtPCR analysis showed that two BRCA1-deficient cell lines, HCC1937 and MDA-MB-436, had 50- to 150-fold greater miR-155 than MDA-MB-231 and MCF7, which both express functional BRCA1 (Fig. 3c,d). Moreover, miR-155 expression analysis in the primary tumors from the *Brca1* conditional knockout mouse model (*Brca1*$^{cko/cko}$;*p53*$^{ko/+}$;*MMTV-Cre*)[35] showed that miR-155 was consistently upregulated in BRCA1-deficient tumors (Fig. 3d; $n = 4$). In contrast, only one of the four tumors from Her2/Neu transgenic mice overexpressed miR-155 (Fig. 3d; $n = 4$). We also observed greater miR-155 expression in mammary epithelial cells (MECs) from *Brca1*$^{cko/cko}$;*K14-Cre* mice compared with MECs from *Brca1*$^{+/+}$;*K14-Cre* mice[36] (Fig. 3e). Also, stable knockdown of *BRCA1* in HEK 293 cells led to greater expression of miR-155 than in wild-type (Fig. 3f). Furthermore, when we transiently expressed wild-type and R1699Q BRCA1 in the BRCA1-deficient breast tumor cell line MDA-MB-436, we found a significant reduction in miR-155 expression only with wild-type BRCA1 (Fig. 3g). We also observed repression of miR-155 expression by wild-type BRCA1 in HCC1937 cells, indicated by dose-dependently increased activity of a luciferase reporter that has miR-155-binding sites at the 3′ untranslated region (UTR; Fig. 3h). Taken together, these results demonstrate that BRCA1 negatively controls miR-155 and that loss of BRCA1 function leads to the upregulation of miR-155.

BRCA1 epigenetically represses miR-155 promoter

Because the biogenesis of miRNAs occurs in multiple steps[37], we examined at which step(s) BRCA1 is involved. In R1699Q embryoid bodies, the primary transcript of *miR-155* gene (pri-miRNA-155) was increased by three-folds compared to (or with?) the WT embryoid bodies (Supplementary Fig. 5a). We also observed that the overexpression of wild-type or R1699Q BRCA1 in BRCA1-deficient MDA-MB-436 cells did not alter the processing of the pri-miR-155 to mature form (Supplementary Fig. 5b). These data suggest that BRCA1 controls miR-155 expression by regulating the transcription of pri-miR-155.

We hypothesized that BRCA1 associates with the miR-155 promoter and suppresses its transcription. Sequence analysis of the mouse miR-155 promoter showed two regions with putative BRCA1-binding sites[38] (BRCA1-1 and BRCA1-2; Supplementary Fig. 6a). Chromatin immunoprecipitation (ChIP) analysis of the promoter using primers (Supplementary Table 5) for these two regions showed that BRCA1 binds to the BRCA1-2 region (Fig. 4a). To further validate this interaction and examine its effect on miR-155

regulation, we carried out mutation analysis. In the BRCA1-2 region, we identified two different clusters of putative BRCA1-binding sites separated by 58 base pairs (Supplementary Fig. 6b). We mutated each of the two putative binding clusters (Mut1 and Mut2) individually and also generated a double mutant (Supplementary Fig. 6c). Each mutant led to miR-155 promoter activation, as measured by a luciferase assay with wild-type BRCA1 in MDA-MD-468 cells (Fig. 4b), suggesting the importance of both binding sites for promoter repression. This is further supported by the observation that the double mutant did not show any additive effect (Fig. 4b). We found that the binding of R1699Q BRCA1 to the miR-155 promoter was comparable to wild-type (Fig. 4a). Thus, we reasoned that BRCA1 may recruit other transcriptional repressors and that the interaction is disrupted without functional BRCA1, leading to derepression of the miR-155 promoter. None of the known co-repressors of BRCA1, including CtIP, COBRA and Myc[39–41], affected BRCA1-dependent repression of miR-155 promoter (data not shown). Furthermore, R1699Q BRCA1 had no effect on the expression of other known transcriptional targets, such as *Gadd45* and *Ccnb1* (also known as *Cyclin B1*) in the mutant embryoid bodies (Supplementary Fig. 6d,e), also suggesting that BRCA1 may regulate miR-155 by a different mechanism.

Because BRCA1 is associated with the histone deacetylase (HDAC) complex[42], we examined the possibility that BRCA1 epigenetically controls miR-155. Treatment with HDAC inhibitors (apicidin, M344 and TSA) in MDA-MB-468 (BRCA1$^+$) led to a two- to four-fold increase of miR-155 (Fig. 4c; data for TSA not shown). In contrast, in the two BRCA1-deficient cell lines, MDA-MB-436 (Fig. 4c) and HCC1937 (Supplementary Fig. 7a, miR-155 expression did not increase in response to the HDAC inhibitors, suggesting that the miR-155 promoter is controlled epigenetically and that the regulation is abrogated without BRCA1. Indeed, luciferase reporter analysis in MDA-MB-468 cells showed a seven- to nine-fold increase in miR-155 promoter activation upon HDAC inhibitor treatment (Fig. 4d). Moreover, the activation of promoters with mutated BRCA1-binding sites decreased after HDAC inhibitor treatment (Fig. 4d), suggesting that BRCA1 is involved in the epigenetic regulation.

On the basis of these results, we further tested whether BRCA1 affects the acetylation of one or more histones on the miR-155 promoter, which in turn could activate or silence the gene. We carried out ChIP analysis using a series of antibodies recognizing acetylated histones and observed that H2A and H3 were more acetylated in BRCA1-deficient MDA-MB-436 cells than in BRCA1$^+$ MCF7 cells (Supplementary Fig. 7b). This higher acetylation of H2A and H3 was also observed in R1699Q embryoid body cells (Fig. 4e), indicating that BRCA1 is responsible for these acetylation changes. Moreover, the acetylation of H2A and H3 was lower when wild-type BRCA1 was expressed in MDA-MB-436 cells, whereas R1699Q overexpression did not have this effect (Fig. 4f). These data demonstrate that BRCA1 negatively controls the miR-155 promoter by decreasing the acetylation of H2A and H3.

To identify the HDAC involved in the deacetylation of histones H2A and H3 at the miR-155 promoter by BRCA1, we carried out ChIP analysis using antibodies to HDAC1–HDAC5 and HDAC7. We observed a specific association between HDAC2 and the miR-155 promoter in cells expressing wild-type BRCA1 (Fig. 4g and Supplementary Fig. 7c). However, in R1699Q cells, HDAC2 association with miR-155 promoter was similar to the IgG control. We tested the interaction between HDAC2 and BRCA1 by coimmunoprecipitation in mouse mammary epithelial cells, and found interaction between HDAC2 and wild-type or M1652I BRCA1 but not between HDAC2 and R1699Q BRCA1 (Fig. 4h).

Because R1699Q BRCA1 associated with the miR-155 promoter but did not interact with HDAC2 (Fig. 4a,h), we questioned whether R1699Q BRCA1 has a dominant-negative effect

on miR-155 regulation. To test this, we coexpressed R1699Q mutant with wild-type BRCA1 in MDA-MB 436 cells and MCF7. R1699Q BRCA1 had no effect on the repression of miR-155 in MDA-MB 436 cells, and miR-155 did not significantly increase upon overexpression of R1699Q BRCA1 in MCF7 cells (Supplementary Fig. 7d), suggesting that R1699Q BRCA1 does not have a dominant-negative effect (see Supplementary Discussion).

Because the mutant miR-155 promoters exhibited higher activity and compromised activation in the presence of HDAC inhibitors (Fig. 4b,d), we tested the association between BRCA1-HDAC2 complex and acetylation of H2A and H3 on the mutant promoters. We transfected wild-type or mutant mouse miR-155 promoter constructs (Mut1, Mut2 and double mutant in Fig. 4b,d) into the BRCA1$^+$ human breast cell line MDA-MB-468, and carried out ChIP analysis. Using mouse promoter–specific primers, we found that wild-type promoter associated with BRCA1 and HDAC2 and led to reduced acetylation of H2A and H3, whereas the mutant promoter (double mutant) did not recruit the BRCA1-HDAC2 complex and, as a result, showed increased acetylation of H2A and H3 (Fig. 4i). On the basis of these observations, we concluded that wild-type BRCA1 can recruit HDAC2 to the miR-155 promoter that deacetylates histones H2A and H3. Notably, using human miR-155 promoter–specific primers, we found that the association between BRCA1-HDAC2 complex and the endogenous human miR-155 promoter is reduced by the presence of exogenous wild-type mouse miR-155 promoter (Fig. 4i) but not by the mutant promoter. This suggests competition for the limited amount of BRCA1-HDAC2 complex (Supplementary Fig. 7e). We also tested three other promoters, *ESRRG*, *CCNB1* and *STAT5A*, with putative BRCA1-binding sites[38], and found no or marginal association of BRCA1 (see Supplementary Discussion). We also observed no change in HDAC2 interaction or histone acetylation (Fig. 4i), suggesting that the epigenetic regulation of miR-155 promoter by BRCA1 is specific.

Effect of miR-155 on tumorigenesis

To examine the effect of overexpression of miR-155 observed in BRCA1 mutant tumors or tumor cell lines, we stably expressed miR-155 in BRCA1$^+$, low miR-155–expressing MDA-MB-468 cells (Supplementary Fig. 8). We then injected control and miR-155-expressing cells into athymic nude mice and monitored tumor growth. Cells overexpressing miR-155 showed accelerated tumor growth relative to control cells (Fig. 5a; $P = 4.12 \times 10^{-4}$, analysis of covariance, ANCOVA). Analysis of individual tumors showed greater miR-155 in tumors from cells overexpressing miR-155 (Supplementary Fig. 8a). This result demonstrates that miR-155 is oncogenic in this breast cancer cell line, consistent with a recent report showing that miR-155 supports the growth of MDA-MB-231 cells[30].

We then tested the effect of miR-155 inhibition in BRCA1-deficient cells on *in vivo* tumor cell growth. We used a mouse BRCA1-deficient tumor cell line (no. 69)[43] with high miR-155 expression, comparable to the HCC1937 cell line (Supplementary Fig. 8b). We generated stable clones (C9 and D6) containing a green fluorescent protein (GFP) reporter construct harboring a miR-155-binding site (miR-sponge; Supplementary Fig. 8c) that exhibited efficient knockdown of miR-155, shown by luciferase reporter assay (Supplementary Fig. 8d). The *in vivo* growth of these clones was significantly lower than the parental cells in an orthotopic transplantation experiment (Fig. 5b,c), demonstrating that the knockdown of miR-155 inhibits *in vivo* tumor growth of BRCA1-deficient cells.

miR-155 upregulation in BRCA1 mutant human breast tumors

To examine the correlation between BRCA1 status and miR-155 expression in human breast cancer, we first analyzed a human breast tumor tissue array. We screened miR-155$^+$ tumors by *in situ* hybridization and found 20 cases showing marked upregulation in a subset of

epithelial cells (on the basis of H&E staining), similar to the staining pattern we observed in embryoid bodies derived from R1699Q ES cells (Fig. 5d and Supplementary Fig. 9a). We also assessed BRCA1 status by immunohistochemistry (Fig. 5d and Supplementary Fig. 9b) and classified the tumors into groups of 50 BRCA1$^+$ tumors and 16 BRCA1-weak or BRCA1$^-$ tumors, which showed background expression of BRCA1. Among 16 tumors with weak or negative BRCA1 expression, 10 were miR-155$^+$ (62.5%). In contrast, only 10 of 50 (20%) BRCA1$^+$ tumors were miR-155$^+$ (Table 1). These results show a significant correlation between loss of BRCA1 and upregulation of miR-155 ($P = 0.022$, Fisher's exact test). We quantified miR-155 expression in 13 of these tumors (3 BRCA1$^+$ and miR-155-low; 10 BRCA1-weak or BRCA1$^-$ and miR-155-high) by rtPCR of miRNA extracted from formaline-fixed, paraffin-embedded (FFPE) sections and found a two- to sixfold upregulation of miR-155 in BRCA1-weak or BRCA1$^-$ tumors compared with BRCA1$^+$ tumors (Supplementary Fig. 10). Next, we examined human tumors with mutation in *BRCA1* (Supplementary Table 6). Of 14 tumors from BRCA1 mutation carriers, 11 (78.5%) had high miR-155 (more than twofold) whereas only 8 of 28 (28%) tumors from noncarriers had high miR-155 ($P = 0.045$ by Fisher's exact test, Fig. 5e). Taken together, our results show that miR-155 upregulation is correlated with BRCA1 mutation in human breast tumors.

DISCUSSION

The R1699Q variant of BRCA1 has shown variable effects in functional, biochemical and biophysical studies and its precise effect on breast cancer risk is unknown[19,44,45]. Therefore, we hypothesized that R1699Q may have a mild to moderate effect on BRCA1 function and is probably a hypomorphic allele. We uncovered a defect in ES cell differentiation caused partially by the upregulation of an oncogenic miRNA, miR-155. Further studies showed that upregulation of miR-155 was associated not only with the R1699Q variant but also with complete loss of BRCA1 function. Interestingly, we observed different levels of miR-155 overexpression in different cell-types, which we attribute to the presence of multiple regulatory signals (see Supplementary Discussion). Because of the oncogenic potential of miR-155, these results suggest that the repression of miR-155 may be a new mode of tumor suppressor function for BRCA1. Our study demonstrates that miR-155 is epigenetically regulated, and that BRCA1 has a role in this regulation via its interaction with the HDAC2 complex (Fig. 5f).

Our study also shows a correlation between loss of BRCA1 function and miR-155 upregulation in human tumors. Future studies may establish whether mir-155 can be used as a potential biomarker to determine the functional status of BRCA1 in tumors (see Supplementary Discussion). The knockdown of miR-155 in BRCA1-deficient cells led to significant reduction in tumor growth. The effectiveness of miR-155 abrogation on growth of established BRCA1-deficient tumors needs to be evaluated in the future to determine the potential use of an anti-miR-155 agent for BRCA1-deficient tumorigenesis.

In conclusion, we characterized the R1699Q mutation and identified a new role for BRCA1 in the epigenetic control of miR-155. We think that functional analysis of other potentially low- or moderate-risk variants of BRCA1 could lead to the discovery of other new biological functions of this multifunctional tumor suppressor that have been masked in variants that severely disrupt the function of BRCA1. For detailed discussion, see Supplementary Discussion

ONLINE METHODS

Antibodies and reagents

For screening of acetylated histones and HDACs, acetyl-histone antibody Sampler kit and HDAC antibody sampler kit (Cell Signaling) were used. To detect BRCA1, two antibodies to BRCA1 were used, E1 (ref. 20) for ChIP and immunoprecipitation and Ab-1 (Calbiochem) for immunohistochemistry and western blots. For further ChIP and coimmunoprecipitation analysis, antibody to acetylated H2A and H3 (Millipore), rabbit monoclonal antibody to HDAC2 (Epitomics) and mouse monoclonal antibody to HDAC2 (Santa Cruz Biotech) were used. Antibody to β-actin was obtained from Santa Cruz Biotechnology. For HDAC inhibition, 1 mM apicidin and M344 (Biovision) and 33 nM trichostatin A (TSA, Sigma) were used. To test the sensitivity to DNA-damaging agents, ES cells were treated with mitomycin C, hydroxyurea and cisplatin at concentrations indicated in Supplementary Figure 2. For luciferase assay of miR-155 promoter reporters and miR-155 reporters, dual luciferase assay reagent (Promega) was used, with pRL-tk as a normalizing reporter.

Generation of R1699Q mutant ES cells

The R1699Q ES cell line was generated from the *Brca1* conditional ES cell line PL2F8 as described[20]. Briefly, Human *BRCA1*-containing BAC DNA harboring the R1699Q mutation and containing a neomycin-resistance gene in the pBACe3.6 vector was electroporated into PL2F8 cells. BAC-containing cells were selected in G-418 (180 μg ml^{-1}) and clones expressing the *BRCA1* transgene were identified by RT-PCR as described[20]. Three RT-PCR-positive clones were expanded and infected with Adeno-Cre virus to remove the conditional *Brca1* allele. Clones undergoing Cre-mediated recombination were selected in HAT-containing media. HAT-resistant ES cell clones were expanded and genotyped by Southern hybridization as described[20].

miRNA expression analysis

The LMT_miRNA_v2 microarray (NCI-Frederick) was designed using the Sanger miR9.0 database (http://www.mirbase.org) and manufactured by Agilent Technologies as custom-synthesized 8 × 15 K microarrays. The total RNA from the embryoid body of wild-type, R1699Q and M1652I BRCA1 at day 7 was labeled using the miRCURY LNA miRNA Array Labeling Kit (Exiqon). The 3′ end of the total RNA was enzymatically labeled with Hy3 and/or Hy5 fluorescent dye (Exiqon) by incubation with T4 RNA ligase at 0 °C for 1 h followed by enzyme inactivation at 65°C for 15 min. The labeled RNA was subsequently used for hybridization onto the microarrays without purification.

ChIP assay

For ChIP assay, cells were fixed with 1% (vol/vol) formaldehyde for 10 min, followed by quenching with 125 mM glycine. Then the cells were lysed in lysis buffer (5 mM HEPES, pH 8.0, 85 mM KCl, 0.5% NP-40 (vol/vol) and protease inhibitors) and nuclei were collected by centrifugation at 2500*g* for 5 min. The nuclei were resuspended in nuclear lysis buffer (50 mM Tris, pH 8.1, 10 mM EDTA, 0.5% (wt/vol) SDS and protease inhibitors) for 20 min (on ice) followed by sonication using 550 Sonic Dismembrator (Fisher Scientific). The debris was cleared by centrifugation and resulting chromatin was five-fold diluted in ChIP dilution buffer (0.01% (wt/vol) SDS, 1.1% (vol/vol) Triton X-100, 1.2 mM EDTA, 16.7 mM Tris, pH 8.1, 167 mM NaCl and protease inhibitors). After preclearing with salmon testis DNA–coated protein G agarose, 1–3 μg antibody was added and incubated overnight. The chromatin-antibody complex was precipitated by protein G agarose and washed extensively by high-salt, low-salt and LiCl wash buffer, respectively[46]. After final

wash with TE, the complex was eluted in 1% (wt/vol) SDS with 0.1 M sodium bicarbonate. The ChIP DNA was recovered by phenol-chloroform extraction and ethanol precipitation with 10 μg yeast tRNA as a carrier.

Quantification of miRNA from the human FFPE tumor samples

Three 6–10 mM sections of FFPE tumors were dissolved in 300 μl of paraffin dissolver (Qiagen). We carried out miRNA purification using miRNeasy FFPE kit (Qiagen) according to the manufacturer's protocol. The miScript Reverse Transcription kit (Qiagen) and miScript SYBR Green PCR kit were used to quantify miR-155 by rtPCR.

miR-155 overexpression and antagomiR experiment

For overexpression of miR-155, MDA-MB-468 cells were transfected with pCMV-pri-miR-155 plasmid with pEGFP-C1 (Clontech). The transfected cells were selected in G-418 (500 μg ml^{-1}) for 7 d. The resulting G-418-resistant cells were collected and used for the injection. To generate antogimiR-155 clone, a plasmid expressing GFP with miR-155-binding site in 3′ UTR was transfected into mouse Brca1-deficient 69 cells. After G-418 selection (500 μg ml^{-1}) for 2 weeks, 96 clones were picked and cultured in a 96-well plate that was further split into three 96-well plates. One of the plates was transfected with miR-155 luciferase reporter plasmid to measure miR-155 expression. Two clones with the highest luciferase activity were selected for further analysis. For *in vivo* growth test, 1×10^6 cells in 100 μl of PBS were injected into the fourth (inguinal) mammary gland of athymic nude mouse (C3H/HeNCr-nu). The growth of tumor was measured after 1 week, followed by measurements on every third day. Tumor volume (in mm^3) was calculated as 2 × length × width.

Statistics

All data are expressed as means ± s.e.m. Differences between two groups were compared using a two-tailed unpaired Student's *t*-test (Microsoft Excel:Mac). $P < 0.05$ was considered statistically significant. For the xenograft experiment, the difference between the two groups (control versus miR-155) was measured by analysis of variance (ANOVA) and ANCOVA using SPSS software. To analyze tumor tissue array data, the Fisher's exact test was used.

Additional methods

Detailed methodology is described in Supplementary Methods.

Supplementary Material

Refer to Web version on PubMed Central for supplementary material.

Acknowledgments

We thank J. Acharya, K. Biswas, R. Chittela, I. Daar, K. Reilly and A. Spurdle for helpful discussions and critical review of the manuscript. We also thank D.M. Livingston (Dana-Farber Cancer Institute) and D.L. Turner (University of Michigan) for providing DNA constructs; D. Swing for help with BAC transgenic mice and allograft experiment; W.D. Foulkes, A. Spurdle, H. Thorne, Y.C. Har, P.S. Yee, A. Saleh, the Georgetown-Lombardi Comprehensive Cancer Center, Familial Cancer and Histopathology and Tissue Share Resources, who helped with the human tumor samples; S. Burkett for cytogenetic analysis; C.H. Kim for microarray analysis and A. Kane and R. Frederickson for illustrations. The research was sponsored by the Center for Cancer Research, US National Cancer Institute and US National Institutes of Health.

References

1. O'Donovan PJ, Livingston DM. BRCA1 and BRCA2: breast/ovarian cancer susceptibility gene products and participants in DNA double-strand break repair. Carcinogenesis. 2010; 31:961–967. [PubMed: 20400477]
2. Venkitaraman AR. Linking the cellular functions of BRCA genes to cancer pathogenesis and treatment. Annu Rev Pathol. 2009; 4:461–487. [PubMed: 18954285]
3. Deng CX. BRCA1: cell cycle checkpoint, genetic instability, DNA damage response and cancer evolution. Nucleic Acids Res. 2006; 34:1416–1426. [PubMed: 16522651]
4. Xia Y, Pao GM, Chen HW, Verma IM, Hunter T. Enhancement of BRCA1 E3 ubiquitin ligase activity through direct interaction with the BARD1 protein. J Biol Chem. 2003; 278:5255–5263. [PubMed: 12431996]
5. Baer R, Ludwig T. The BRCA1/BARD1 heterodimer, a tumor suppressor complex with ubiquitin E3 ligase activity. Curr Opin Genet Dev. 2002; 12:86–91. [PubMed: 11790560]
6. Bork P, et al. A superfamily of conserved domains in DNA damage-responsive cell cycle checkpoint proteins. FASEB J. 1997; 11:68–76. [PubMed: 9034168]
7. Abbott DW, et al. BRCA1 expression restores radiation resistance in BRCA1-defective cancer cells through enhancement of transcription-coupled DNA repair. J Biol Chem. 1999; 274:18808–18812. [PubMed: 10373498]
8. Li S, et al. Binding of CtIP to the BRCT repeats of BRCA1 involved in the transcription regulation of p21 is disrupted upon DNA damage. J Biol Chem. 1999; 274:11334–11338. [PubMed: 10196224]
9. Cantor SB, et al. BACH1, a novel helicase-like protein, interacts directly with BRCA1 and contributes to its DNA repair function. Cell. 2001; 105:149–160. [PubMed: 11301010]
10. Yu X, Chini CC, He M, Mer G, Chen J. The BRCT domain is a phospho-protein binding domain. Science. 2003; 302:639–642. [PubMed: 14576433]
11. Cortez D, Wang Y, Qin J, Elledge SJ. Requirement of ATM-dependent phosphorylation of brca1 in the DNA damage response to double-strand breaks. Science. 1999; 286:1162–1166. [PubMed: 10550055]
12. Ruffner H, Jiang W, Craig AG, Hunter T, Verma IM. BRCA1 is phosphorylated at serine 1497 *in vivo* at a cyclin-dependent kinase 2 phosphorylation site. Mol Cell Biol. 1999; 19:4843–4854. [PubMed: 10373534]
13. Chen J. Ataxia telangiectasia-related protein is involved in the phosphorylation of BRCA1 following deoxyribonucleic acid damage. Cancer Res. 2000; 60:5037–5039. [PubMed: 11016625]
14. Ouchi M, et al. BRCA1 phosphorylation by Aurora-A in the regulation of G2 to M transition. J Biol Chem. 2004; 279:19643–19648. [PubMed: 14990569]
15. Szabo CI, King MC. Inherited breast and ovarian cancer. Hum Mol Genet. 1995; 4(Spec No): 1811–1817. [PubMed: 8541881]
16. Williams RS, Lee MS, Hau DD, Glover JN. Structural basis of phosphopeptide recognition by the BRCT domain of BRCA1. Nat Struct Mol Biol. 2004; 11:519–525. [PubMed: 15133503]
17. Clapperton JA, et al. Structure and mechanism of BRCA1 BRCT domain recognition of phosphorylated BACH1 with implications for cancer. Nat Struct Mol Biol. 2004; 11:512–518. [PubMed: 15133502]
18. Lovelock PK, et al. Identification of BRCA1 missense substitutions that confer partial functional activity: potential moderate risk variants? Breast Cancer Res. 2007; 9:R82. [PubMed: 18036263]
19. Gómez García EB, et al. A method to assess the clinical significance of unclassified variants in the BRCA1 and BRCA2 genes based on cancer family history. Breast Cancer Res. 2009; 11:R8. [PubMed: 19200354]
20. Chang S, Biswas K, Martin BK, Stauffer S, Sharan SK. Expression of human BRCA1 variants in mouse ES cells allows functional analysis of BRCA1 mutations. J Clin Invest. 2009; 119:3160–3171. [PubMed: 19770520]
21. Tam W, Hughes SH, Hayward WS, Besmer P. Avian bic, a gene isolated from a common retroviral site in avian leukosis virus-induced lymphomas that encodes a noncoding RNA,

cooperates with c-myc in lymphomagenesis and erythroleukemogenesis. J Virol. 2002; 76:4275–4286. [PubMed: 11932393]

22. van den Berg A, et al. High expression of B-cell receptor inducible gene BIC in all subtypes of Hodgkin lymphoma. Genes Chromosom Cancer. 2003; 37:20–28. [PubMed: 12661002]
23. Metzler M, Wilda M, Busch K, Viehmann S, Borkhardt A. High expression of precursor microRNA-155/BIC RNA in children with Burkitt lymphoma. Genes Chromosom Cancer. 2004; 39:167–169. [PubMed: 14695998]
24. Kluiver J, et al. BIC and miR-155 are highly expressed in Hodgkin, primary mediastinal and diffuse large B cell lymphomas. J Pathol. 2005; 207:243–249. [PubMed: 16041695]
25. O'Connell RM, et al. Sustained expression of microRNA-155 in hematopoietic stem cells causes a myeloproliferative disorder. J Exp Med. 2008; 205:585–594. [PubMed: 18299402]
26. Costinean S, et al. Pre-B cell proliferation and lymphoblastic leukemia/high-grade lymphoma in E(mu)-miR155 transgenic mice. Proc Natl Acad Sci USA. 2006; 103:7024–7029. [PubMed: 16641092]
27. Yamamoto M, et al. miR-155, a Modulator of FOXO3a protein expression, is underexpressed and cannot be upregulated by stimulation of HOZOT, a line of multifunctional Treg. PLoS ONE. 2011; 6:e16841. [PubMed: 21304824]
28. Kong W, et al. MicroRNA-155 regulates cell survival, growth, and chemosensitivity by targeting FOXO3a in breast cancer. J Biol Chem. 2010; 285:17869–17879. [PubMed: 20371610]
29. Gironella M, et al. Tumor protein 53-induced nuclear protein 1 expression is repressed by miR-155, and its restoration inhibits pancreatic tumor development. Proc Natl Acad Sci USA. 2007; 104:16170–16175. [PubMed: 17911264]
30. Jiang S, et al. MicroRNA-155 functions as an OncomiR in breast cancer by targeting the suppressor of cytokine signaling 1 gene. Cancer Res. 2010; 70:3119–3127. [PubMed: 20354188]
31. Kanellopoulou C, et al. Dicer-deficient mouse embryonic stem cells are defective in differentiation and centromeric silencing. Genes Dev. 2005; 19:489–501. [PubMed: 15713842]
32. Deffenbaugh AM, Frank TS, Hoffman M, Cannon-Albright L, Neuhausen SL. Characterization of common BRCA1 and BRCA2 variants. Genet Test. 2002; 6:119–121. [PubMed: 12215251]
33. Iorio MV, et al. MicroRNA gene expression deregulation in human breast cancer. Cancer Res. 2005; 65:7065–7070. [PubMed: 16103053]
34. Volinia S, et al. A microRNA expression signature of human solid tumors defines cancer gene targets. Proc Natl Acad Sci USA. 2006; 103:2257–2261. [PubMed: 16461460]
35. Brodie SG, et al. Multiple genetic changes are associated with mammary tumorigenesis in Brca1 conditional knockout mice. Oncogene. 2001; 20:7514–7523. [PubMed: 11709723]
36. Liu X, et al. Somatic loss of BRCA1 and p53 in mice induces mammary tumors with features of human BRCA1-mutated basal-like breast cancer. Proc Natl Acad Sci USA. 2007; 104:12111–12116. [PubMed: 17626182]
37. Bartel DP. MicroRNAs: genomics, biogenesis, mechanism, and function. Cell. 2004; 116:281–297. [PubMed: 14744438]
38. Cable PL, et al. Novel consensus DNA-binding sequence for BRCA1 protein complexes. Mol Carcinog. 2003; 38:85–96. [PubMed: 14502648]
39. Aiyar SE, Cho H, Lee J, Li R. Concerted transcriptional regulation by BRCA1 and COBRA1 in breast cancer cells. Int J Biol Sci. 2007; 3:486–492. [PubMed: 18071589]
40. Yu X, Wu LC, Bowcock AM, Aronheim A, Baer R. The C-terminal (BRCT) domains of BRCA1 interact *in vivo* with CtIP, a protein implicated in the CtBP pathway of transcriptional repression. J Biol Chem. 1998; 273:25388–25392. [PubMed: 9738006]
41. Wang Q, Zhang H, Kajino K, Greene MI. BRCA1 binds c-Myc and inhibits its transcriptional and transforming activity in cells. Oncogene. 1998; 17:1939–1948. [PubMed: 9788437]
42. Yarden RI, Brody LC. BRCA1 interacts with components of the histone deacetylase complex. Proc Natl Acad Sci USA. 1999; 96:4983–4988. [PubMed: 10220405]
43. Wang RH, et al. Interplay among BRCA1, SIRT1, and Survivin during BRCA1-associated tumorigenesis. Mol Cell. 2008; 32:11–20. [PubMed: 18851829]

44. Lee MS, et al. Comprehensive analysis of missense variations in the BRCT domain of BRCA1 by structural and functional assays. Cancer Res. 2010; 70:4880–4890. [PubMed: 20516115]
45. Rowling PJ, Cook R, Itzhaki LS. Toward classification of BRCA1 missense variants using a biophysical approach. J Biol Chem. 2010; 285:20080–20087. [PubMed: 20378548]
46. Shang Y, Hu X, DiRenzo J, Lazar MA, Brown M. Cofactor dynamics and sufficiency in estrogen receptor-regulated transcription. Cell. 2000; 103:843–852. [PubMed: 11136970]

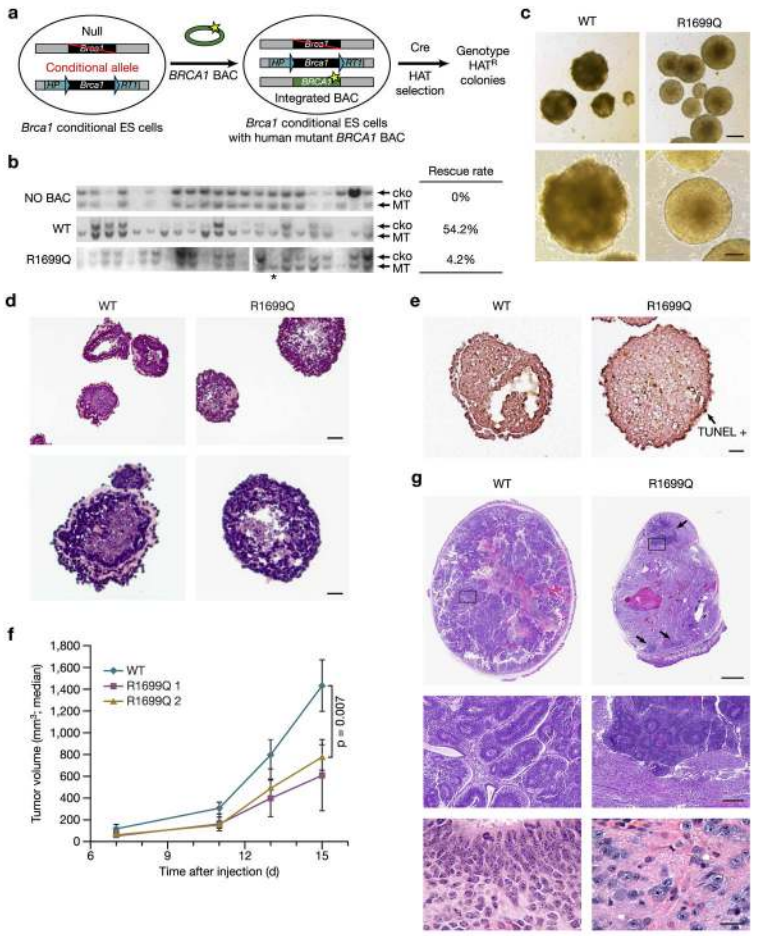

Figure 1.

R1699Q mutant ES cells show reduced survival and differentiation defects. (**a**) Schematics of generation of R1699Q ES cells using PL2F8 cells containing a null and a conditional allele of *Brca1*. Two halves of human *HPRT1* minigenes (HP and RT) flanking the two loxP sites (shaded triangles) of the conditional allele. Cre recombinants are HAT resistant (HAT^R). (**b**) Southern hybridization of HAT^R colonies from experiments without BAC (NO BAC), wild-type (WT) *BRCA1* BAC and R1699Q BRCA1 BAC. Bottom band, null allele (MT); top band, conditional allele (cko). Rescue rate, percentage $Brca1^{ko/ko}$ clones. Asterisk, $Brca1^{ko/ko}$ ES cell. (**c**) Whole mount of embryoid bodies generated from ES cells expressing wild-type (left) and R1699Q (right) BRCA1 at day 14 in culture. Bottom, higher magnification of embryoid bodies. Scale bar, 50 μm, top; 20 μm, bottom. (**d**) H&E staining of embryoid bodies generated from ES cells expressing wild-type (left) and R1699Q (right) BRCA1 at day 14 in culture. Scale bar, 100 μm, top; 50 μm, bottom. (**e**) TUNEL staining of embryoid bodies. Arrow, $TUNEL^+$ cells. Scale bar, 50 μm. (**f**) Teratoma growth of one wild-type and two R1699Q clones were examined in mice ($n = 5$ for each group). Values are means ± s.e.m. ($P = 0.007$). (**g**) H&E staining of teratomas dissected 15 d after injection. Top, section of the whole teratoma; middle, magnified images of the regions indicated at top. Arrows, neurorosette structures. Bottom, neural cells immature in wild-type (left) and more differentiated in R1699Q (right) teratomas. Scale bar, 2 μm, top; 0.2 μm, middle; 50 μm, bottom.

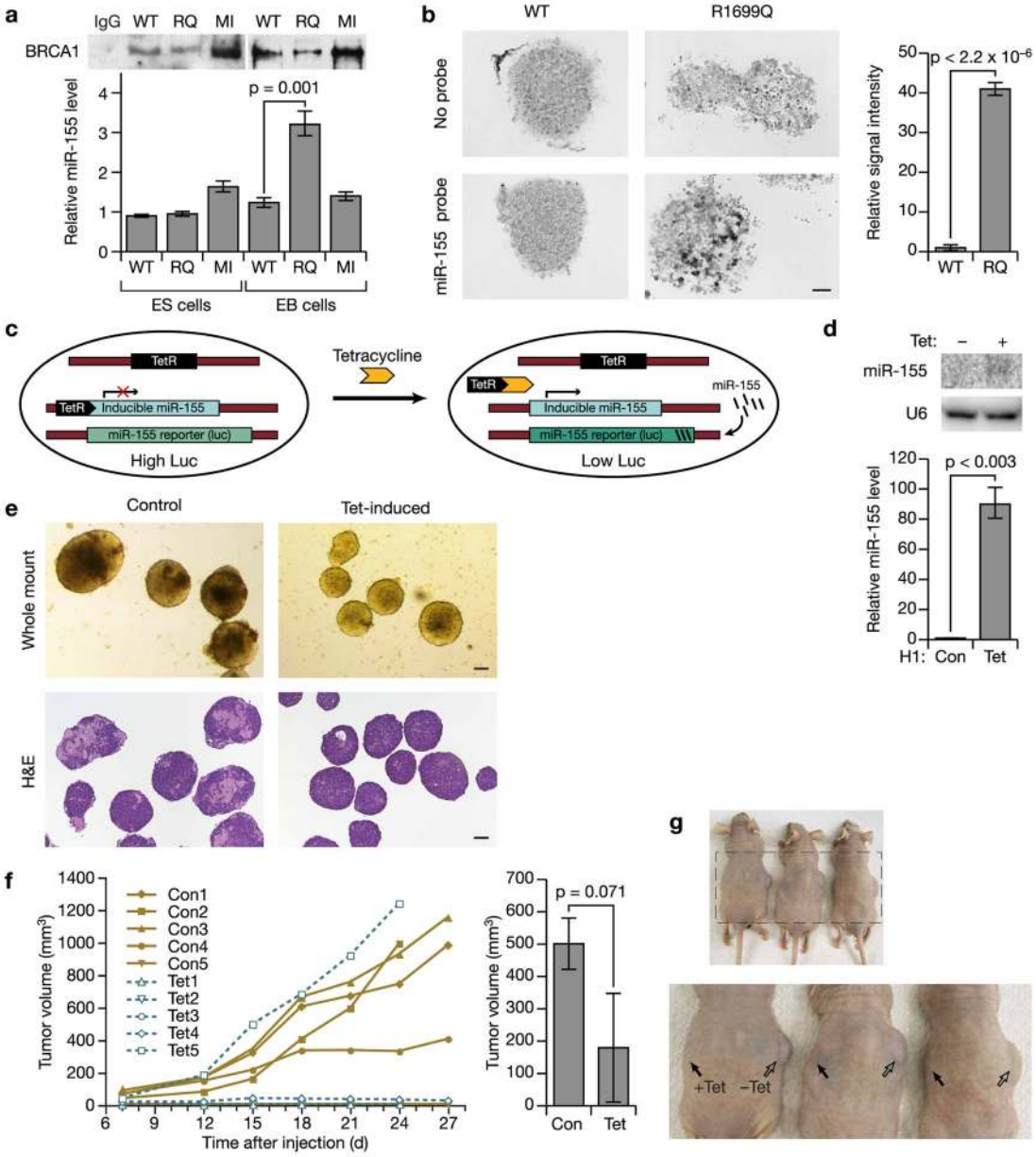

Figure 2.

Identification of miR-155 upregulation in R1699Q mutant cells and its effect on ES cell differentiation. (**a**) Quantification of miR-155 by rtPCR in wild-type (WT), R1699Q (RQ) and M1652I (MI) ES cells and embryoid bodies (EB cells) on day 7 of culture. U6 small nuclear RNA (snRNA) was used for normalization. Top, BRCA1 protein expression. (**b**) Representative pictures of miR-155 *in situ* hybridization in wild-type and R1699Q embryoid bodies using DIG-labeled antisense LNA of miR-155. Top, no-probe controls showing background signal (scale bar, 50 μm). Right, relative average signal. Error bar = s.d. (**c**) Schematic of miR-155 inducible system in ES cells. miR-155 is induced by tetracycline, which then represses the luciferase reporter (luc) containing miR-155-binding sites at the 3′ end. (**d**) miR-155 overexpression in ES cells after tetracycline (tet) induction, with U6 snRNA as control. Top, overexpression by northern hybridization; bottom, quantification by

rtPCR. Error bar = s.d. (**e**) Representative pictures of embryoid bodies generated from wild-type ES cells with induced expression of miR-155. Top, whole mount of embryoid bodies; bottom, H&E-stained sections. Scale bar, 100 μm. (**f**) Teratoma growth of wild-type ES cells with (Tet1–Tet5) and without (Con1–Con5) miR-155 induction. Left, teratoma growth. Right, average tumor volume on day 18 after injection. Minimum value of each group was excluded ($n = 4$; values are means ± s.e.m.). (**g**) Representative picture of teratomas in mice injected with control cells (−Tet, right) and Tet-induced cells (+Tet, left). Bottom, enlarged view.

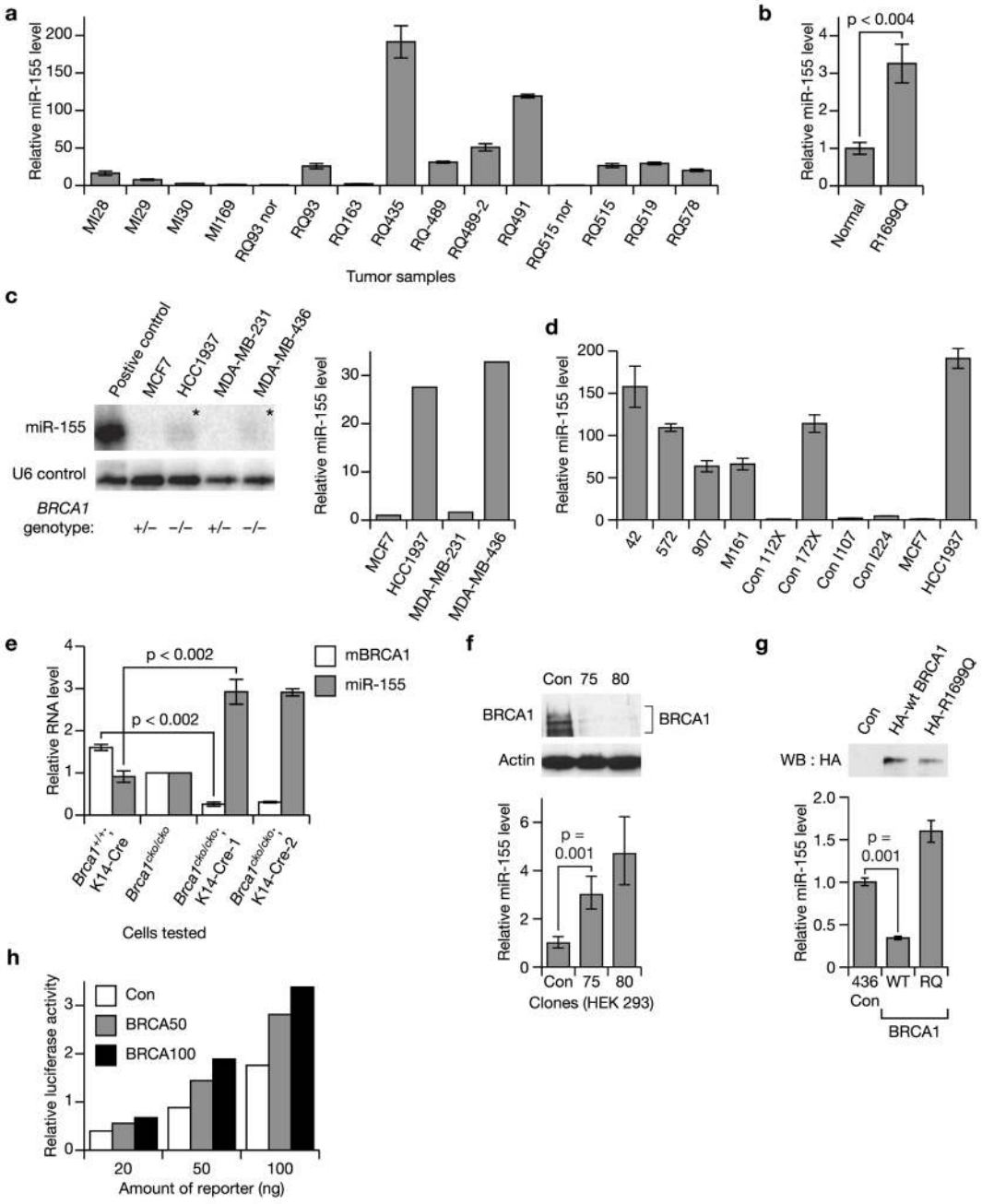

Figure 3.

BRCA1 negatively controls miR-155 expression. (**a**) Quantification of miR-155 in tumors from the *Brca1*$^{ko/+}$;*Trp53*$^{ko/+}$;*Tg*^{R1699Q} mice (RQ, $n = 9$). Normal liver (RQ93 nor), mammary gland (RQ515 nor) and tumors from *Brca1*$^{ko/+}$;*Trp53*$^{ko/+}$;*Tg*^{M1652I} mice (MI, $n = 4$) used as control. (**b**) Quantification of miR-155 in a breast tumor from an R1699Q mutation carrier. Normal, normal breast tissue. (**c**) Expression analysis of miR-155 by northern hybridization in four human breast cancer cell lines of different *BRCA1* genotypes. Positive control, HEK293 cell line overexpressing miR-155; loading control, U6 snRNA; asterisk, miR-155 signal. Right, quantification of signal, normalized by U6 snRNA. (**d**) rtPCR of miR-155 in four *Brca1* deficient tumors (42, 572, 907 and M161) from

Brca1$^{cko/cko}$;*p53*$^{ko/+}$;*MMTV Cre* mice and four tumors (Con 112X, Con 172X, Con I107 and Con I224) from Her2/Neu transgenic mice. MCF7 and HCC1937 were negative and positive control, respectively. (**e**) rtPCR of miR-155 in MECs from two *Brca1*$^{cko/cko}$;*K14 Cre* mice. Control, MECs from K14 Cre only and *Brca*$^{cko/cko}$. (**f**) Knockdown of BRCA1 in two clones (75 and 80) of HEK293 cells stably expressing *BRCA1* short hairpin RNA (top). Loading control, β-actin (middle). Bottom, rtPCR quantification of miR-155 in the BRCA1 knockdown clones (75 and 80). Con, control. (**g**) Real-time quantification of miR-155 after ectopic expression of wild-type (WT) or R1699Q BRCA1 in BRCA1-deficient MDA-MB-436 cells. Top, expression of wild-type and R1699Q BRCA1. (**h**) miR-155 reporter assay in BRCA1-deficient HCC1937 cells using increasing amounts of wild-type *BRCA1* cDNA (Con, untransfected cells and BRCA50, 50 ng; BRCA100, 100 ng. Error bar = s.d.

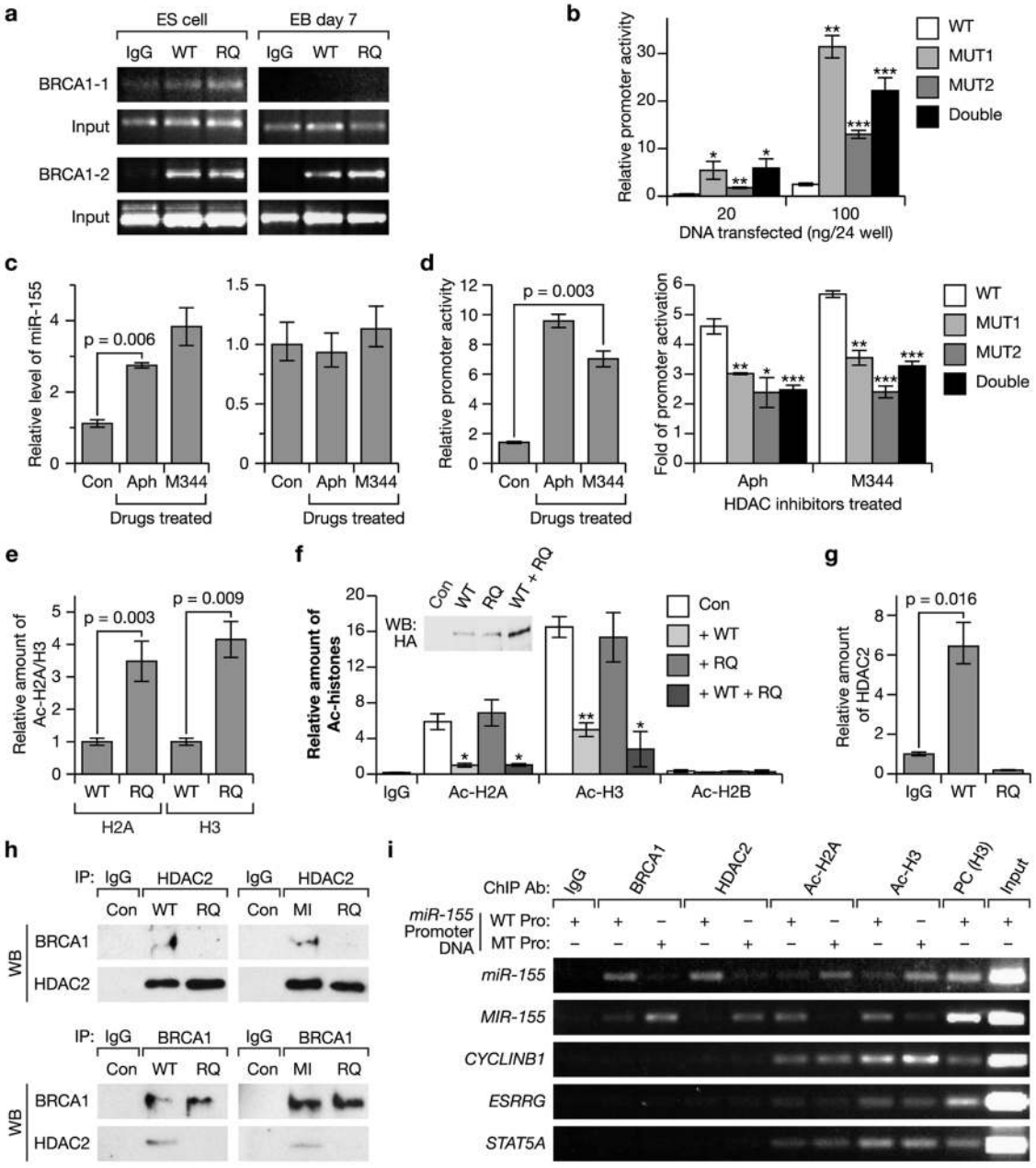

Figure 4.

Mechanism of miR-155 repression by BRCA1. (**a**) Binding of BRCA1 to miR-155 promoter at two potential regions (BRCA1-1 and BRCA1-2). ES cells and embryoid bodies (EB) at day 7 in culture with wild-type and R1699Q (RQ). BRCA1 by ChIP assay. Input, 5% of total chromatin. (**b**) Effect of mutation of putative BRCA1-binding sites (Mut1, Mut2 or double mutant) on miR-155 promoter activation measured by luciferase assay (*$P < 0.05$, **$P < 0.01$, ***$P < 0.005$). (**c**) Effect of HDAC inhibitors on miR-155 expression measured by rtPCR in BRCA1^{+} MDA-MB-468 (left) and BRCA1-deficient MDA-MB-436 cells (right). Con, no treatment; Aph, apicidin. (**d**) Effect of HDAC inhibitors on wild-type miR-155 promoter (left) and mutant promoter (right) activation in MDA-MB-468 cells measured by luciferase assay (*$P < 0.02$, **$P < 0.01$, ***$P < 0.005$). Con, no treatment;

Aph, apicidin. (**e**) ChIP assay to quantify acetylation level of histones H2A and H3 on miR-155 promoter, in wild-type and R1699Q EB cells by rtPCR. (**f**) Effect of wild-type, RQ and wild-type + RQ BRCA1 on acetylation of histones H2A and H3 on miR-155 promoter in MDA-MB-436 cells measured by ChIP assay and rtPCR. Con, transfection with vector only (*$P < 0.02$, **$P < 0.01$). Western blot (WB) analysis of ectopic protein expression using antibody to hemagglutinin (HA). (**g**) Association of HDAC2 on miR-155 promoter in wild-type and R1699Q EB cells analyzed by ChIP assay and rtPCR. IgG, negative control. (**h**) Co-immunoprecipitation (Co-IP) between HDAC2 and wild-type or M1652I or R1699Q BRCA1 in MECs from mice with wild-type or R1699Q BAC transgenes (left) or M1652I transgene (right). Top panels, IP with HDAC2 antibody; bottom panels IP with human-specific BRCA1 antibody. (**i**) MDA-MB 468 cells transfected with luciferase reporter plasmid with mouse wild-type or double mutant (MT) miR-155 promoter (pro). ChIP assay was carried out with indicated antibodies (Ab). Association of BRCA1-HDAC2 complex and acetylation of histones H2A and H3 on transfected mouse miR-155 promoter (*mir155*, top) and endogenous miR-155 promoter (*MIR155* to test competition effect. BRCA1 binding on *ESRRG*, *CCNB1* and *STAT5A* promoters with putative binding sites. Error bar = s.d.

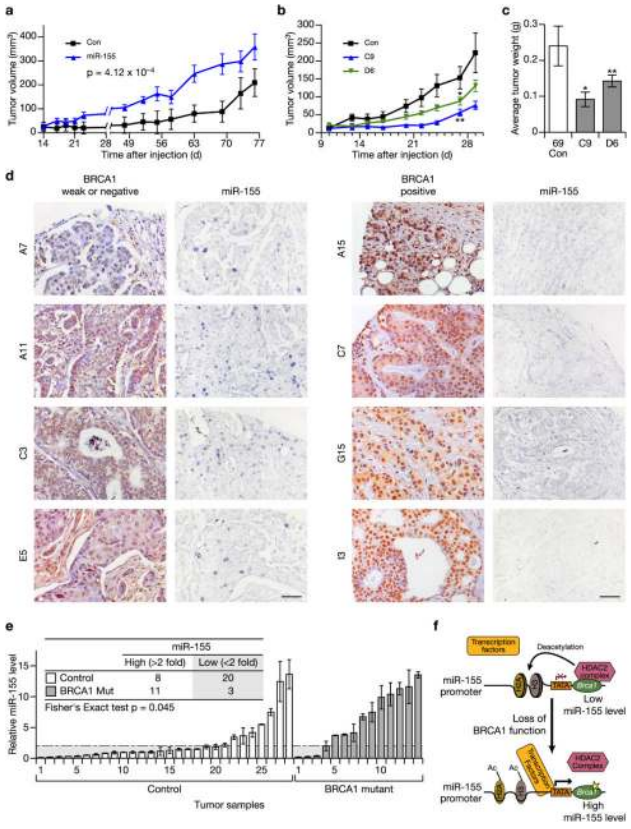

Figure 5.

Physiological relevance of miR-155 upregulation in BRCA1-deficient tumors. (**a**) Xenograft tumor growth of MDA-MB-468 cells with stable expression of miR-155 ($P = 4.12 \times 10^{-4}$, ANCOVA test). Values are mean ± s.e.m. (**b**) Growth of two clones (C9 and D6) with miR-155 stable knockdown and the parental cells (Con) orthotropically transplantated in mice (values are means ± s.e.m., $*P = 0.031$, $**P = 0.025$). (**c**) Average mass of tumors in **b** (values are means ± s.e.m.). (**d**) Representative pictures of 66 human breast tumors in tumor tissue microarray probed with antibody to BRCA1 (Ab-1) or mouse IgG (negative control) and DIG-labeled antibody to miR-155. Scale bar, 50 μm. (**e**) rtPCR quantification of miR-155 in 28 tumors from non-BRCA1 controls and 14 tumors from BRCA1 mutation (mut) carriers (see Supplementary Table 6 for mutation description). *RNU5A* was used for normalization. Shaded area, low miR-155 based on two-fold cut-off (dashed horizontal line). Text box, number of miR-155 high and low tumors in each group. (**f**) Schematic of role for BRCA1 in epigenetic control of miR-155 promoter. In wild-type BRCA1–containing cells, miR-155 is silenced by the BRCA1-HDAC2 complex, which deacetylates H2A and H3 histones. Without functional BRCA1, the interaction of BRCA1-HDAC2 complex is disrupted, which in turn increases acetylated (Ac) H2A and H3, which activates the miR-155 promoter.

Table 1

Summary of tumor tissue array analysis

Number of tumors analyzed (66)			
BRCA1$^+$ (50)		**BRCA1-weak or BRCA1$^-$ (16)**	
miR-155$^+$	miR-155$^-$	miR-155$^+$	miR-155$^-$
10 (20.0%)	40 (80.0%)	10 (62.5%)*	6 (37.5%)

*P = 0.022, Fisher's exact test.